An oblique effect for local motion: Psychophysics and natural movie statistics

Steven C. Dakin Institute of Ophthalmology, University College London, Bath Street, London, United Kingdom

Isabelle Mareschal Institute of Ophthalmology, University College London, Bath Street, London, United Kingdom

Peter J. Bex Institute of Ophthalmology, University College London, Bath Street, London, United Kingdom

Human perception of visual motion is thought to involve two stages—estimation of local motion (i.e., of small features) and global motion (i.e., of larger objects)—identified with cortical areas V1 and MT, respectively. We asked if poor discrimination of oblique compared to cardinal directions (the oblique effect for motion; OEM) reflects a deficit in local or in global motion processing. We used an equivalent noise (EN) paradigm—where one measures direction discrimination thresholds in the presence of directional variability—to quantify local and global limits. We report that the OEM diminishes with increasing directional variability, indicating that global motion processing (the number of local motion signals pooled) is equal across all directions and that the OEM is attributable to anisotropies in local motion processing. To investigate the origin of this effect, we measured local motion statistics from natural movies (filmed from the point of view of a walking observer). This analysis reveals that the distribution of local directional energy on the oblique directions tends to be broader, and frequently more asymmetric, than on the cardinal directions. If motion detectors are optimized to deal with our visual world then such anisotropies likely explain the local nature of the OEM.

Keywords: equivalent noise, local/global processing, motion, natural scenes, oblique effect

Introduction

The *oblique effect* refers to observers' superior psychophysical performance with static or moving stimuli presented on the cardinal (vertical and horizontal) compared to the oblique meridia (Appelle, 1970). Contrast detection thresholds for stimuli moving in oblique directions are elevated, as are direction discrimination thresholds for high-contrast stimuli, although motion coherence thresholds (the minimum number of non-randomly moving dots supporting direction discrimination) are similar across all directions of motion (Gros, Blake, & Hiris, 1998). A number of theories have been advanced to account for the oblique effect: oblique channels could be more broadly tuned, more asymmetrically tuned, or more noisy than their cardinal counterparts. In terms of the neural substrate for the phenomenon, there is evidence for both a reduction in the number of neurons that are selective to oblique orientations as well as a broadening of their bandwidth (Li, Peterson, & Freeman, 2003). Evidence from an fMRI study (Furmanski & Engel, 2000) indicates that oblique stimuli lead to lower activity in cortical area V1 but not in later areas suggesting that response gain can compensate for lower sensitivity in early stages. This is of interest in considering the oblique effect for motion (OEM) in that human motion perception is thought to involve two stages. The first is the estimation of local direction over a small area and is thought to be carried out by cells in cortical area V1. The second involves pooling these signals across space to estimate overall or global direction; this pooling has been linked to the operation of area MT. Thus, if the oblique effect is generally caused by a difference in processing in V1 then the OEM should primarily be associated with local motion perception.

We addressed the role of local and global motion processing in the OEM using an equivalent noise (EN) paradigm (Barlow, 1980; Dakin, Mareschal, & Bex, 2005; Heeley, Buchanan-Smith, Cromwell, & Wright, 1997; Watamaniuk & Heinen, 1999; Watt & Morgan, 1983). The paradigm is illustrated in Figure 1. EN relies on the idea that a psychophysically measured threshold results from the sum of both internal and external noise. Given that observers' thresholds are estimates of response variability, and that external noise imposed onto the stimulus can also be expressed in terms of variability, EN uses a variance summation model to quantify observers' performance, in terms of (a) external noise imposed on the stimulus, (b) sample size

doi: 10.1167/5.10.9 Received June 14, 2005; published December 16, 2005 ISSN 1534-7362

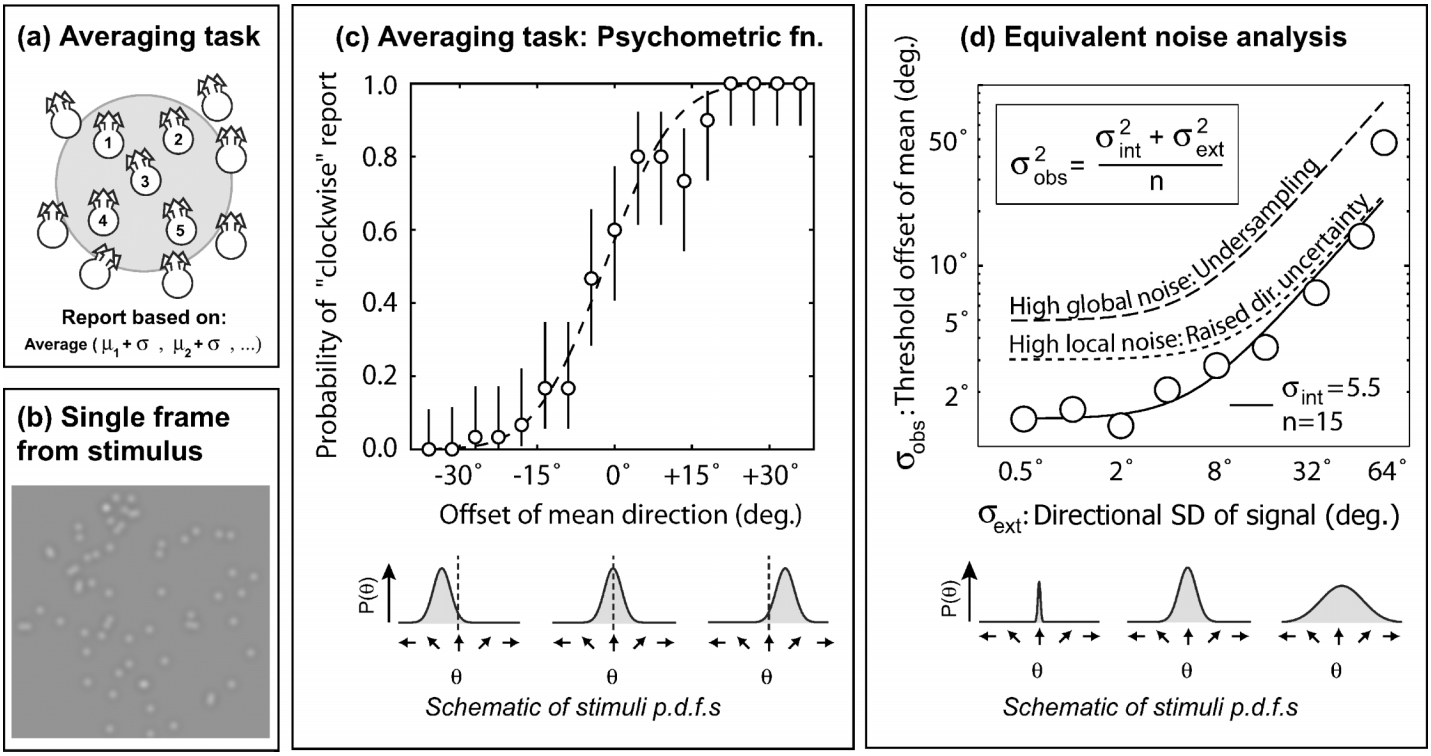

Figure 1. (a) Our ability to judge the overall direction of several elements is limited both by global factors (the number of directions combined-shaded region) and by local factors (the precision of each direction estimate-multiple arrowheads). (b) Stimuli consist of a patch of drifting spatially band-pass elements. (c) Observers report if the average direction (of elements moving with Gaussian-distributed directions) is clockwise or anti-clockwise of a reference. We measure the probability of a ''clockwise'' report for various offsets in mean direction and use the slope of the best-fitting wrapped cumulative Gaussian function as the threshold offset in mean direction. We then separate the influence of local and global factors on this judgment using an equivalent noise paradigm. (d) Plotting threshold as a function of the range of directions present in the stimulus, observers' performance (open circles) is good when directional *SD* is low and deteriorates as it increases. Because we are estimating response variability as a function of stimulus variability, EN exploits additivity of variance to model the data (boxed equation) in terms of external noise (the directional range; σ_{ext}) and local (σ_{int}) and global (n) limits on integration. For the example shown, the observer pooled ~15 local direction estimates, each with a precision of 5.5°. The signatures of poorer local or global processing are also illustrated.

(globally pooled), and (c) precision with each sample can be estimated (local noise).

Methods

Apparatus

Experiments were run under MATLAB (MathWorks Ltd.) using elements of the PsychToolobox (Brainard, 1997). Stimuli were presented on a CRT monitor fitted with a video attenuator that had been modified to generate gray scale images. The display (a La Cie Electron Blue 22" monitor) was calibrated with a Minolta LS110 photometer and linearized in software to give pseudo 12-bit contrast accuracy. The display had a mean background luminance of 50 cd/m^2.

Stimuli

Stimuli were circular patches (4.0 deg. radius) containing 64 moving, spatially band-pass (Laplacian-of-Gaussian; $\nabla^2 G$) micro-patterns defined as:

$$\nabla^2 G(x,y) = \frac{x^2+y^2-2\sigma^2}{2\pi\sigma^6}\exp\left(-\frac{x^2+y^2}{2\sigma^2}\right). \quad (1)$$

The value of σ was fixed at 7.6 arcmin producing a patch with a peak spatial frequency of 1.78 c/deg. Movies were 480 ms sequences played at the monitor refresh rate (75 Hz). Each of 12 unique movie frames was repeated three times before being updated. Elements moved in discrete jumps of 12 arcmin (i.e., approximately 35% of one cycle of the peak s.f. of the patch per frame),

corresponding to a speed of approximately 5 deg/sec and were positioned with subpixel accuracy (within 10% of one pixel). All elements were of "infinite lifetime"; if an element passed outside of the viewable aperture, its position was wrapped to the opposite side.

Elements moved with directions drawn from a wrapped normal (WN) distribution, defined on the range $\theta \epsilon (0, 2\pi)$ by the probability density functions:

$$f(\theta) = \frac{1}{\sigma\sqrt{2\pi}} \sum_{k=-\infty}^{k=\infty} \exp\left[\frac{-(\theta - \mu - 2\pi k)^2}{2\sigma^2}\right]. \quad (2)$$

This function has no closed form but can be evaluated using a minimization procedure (see Dakin et al., 2005).

Subjects

The three authors (wearing optical correction as necessary) served as observers. All are experienced at psychophysical tasks involving motion perception and conducted practice runs until their performance reached asymptotic levels.

Procedure

Subjects judged whether the overall direction of a field of moving, band-pass elements was clockwise or counterclockwise of a reference direction; auditory feedback was given for incorrect responses. We tested several reference directions. In the first condition (full EN), we used either vertical–upwards motion (a cardinal direction) or "upwards and to the left" (oblique) motion and in the second (high–low variance) condition, we used from 0° to 337.5° in steps of 22. 5°. The reference direction was indicated by crosshairs that were continuously present on the screen. For the EN condition, directions were drawn from WN distributions with *SD*s of 0.5°, 1°, 2°, 4°, 8°, 16°, 32°, 64°, or 90°. In the high–low variance condition we tested only 0.5° and 32°. From trial-to-trial, the mean direction of the distribution was determined by the method of constant stimuli which tested 17 evenly spaced directions (one at the reference level plus 8 clockwise and 8 counterclockwise relative to reference) that bracketed the psychometric function adequately for the direction–range condition being tested (this range was determined using pilot runs of an adaptive method of constant stimuli; Watt & Andrews, 1981). At least two blocks of 272 trials were undertaken for each subject in all conditions. Raw data were fit with wrapped cumulative Gaussian functions using a bootstrapping procedure. Error bars on all plots indicate 95% confidence intervals on the estimated slope of these fits.

Results

Figure 2a plots discrimination thresholds for three observers' judgment of overall direction (clockwise or anti-clockwise of reference) as a function of the range of directions present in the stimulus, and for two reference directions (vertical and 45°). At low levels of directional variability observers are consistently worse at judging the direction of stimuli moving in near-oblique directions—this is the OEM. However, performance converges, and the OEM effectively disappears at high levels of directional variance. The fits from the EN analysis, shown by the solid lines, provide a good account of performance in both conditions. Parameters from the fits (shown in the legends of Figure 2a) reveal that this pattern of performance is consistent with observers pooling a constant number of local directions (n) in making their judgments of global direction but being approximately twice as uncertain about the direction of individual elements (σ_{int}) moving in near-oblique directions than those moving in near-cardinal directions.

To determine if the OEM is generally reduced at high directional *SD*s, we next measured direction discrimination for a range of reference directions "around the clock" either at a single low or a single high level of directional noise. Results are presented in Figures 2b and c for the low and high directional *SD* conditions, respectively (note that there is no reflection of data in these plots). The pattern of thresholds around 360° produced "fat crosses" in Figure 2b and indicates a robust oblique effect for all noncardinal directions tested (i.e., beyond 22.5° of the cardinals). In contrast, the oblique effect was greatly reduced when measured with a broad range of directions present in the stimulus (Figure 2c). Results were not uniformly equal around the clock (e.g., PJB shows a general advantage for downwards motion), but given the degree of variability in threshold estimates (error bars indicate 95% confidence intervals) our findings are consistent with the results from the first part of the experiment: the OEM is attributable to observers being less precise at judging the direction of any one element (higher internal noise), rather than being poor at judging the direction of the field as a whole. Our findings are also consistent with an earlier report (in abstract form) of a general reduction in the extent of the oblique effect with the addition of directional noise (Flinn & Watamaniuk, 1997).

There is increasing consensus that the human visual system is optimized for characteristics of the natural visual environment (e.g., Field, 1987) and it is known that there is an overrepresentation of information on the cardinal axes in static images (Baddeley & Hancock, 1991; Betsch, Einhauser, Kording, & Konig, 2004; Coppola, Purves, McCoy, & Purves, 1998; Craven, 1993; Hancock, Baddeley, & Smith, 1992; Hansen, Essock, Zheng, & DeFord, 2003; Keil & Cristobal, 2000;

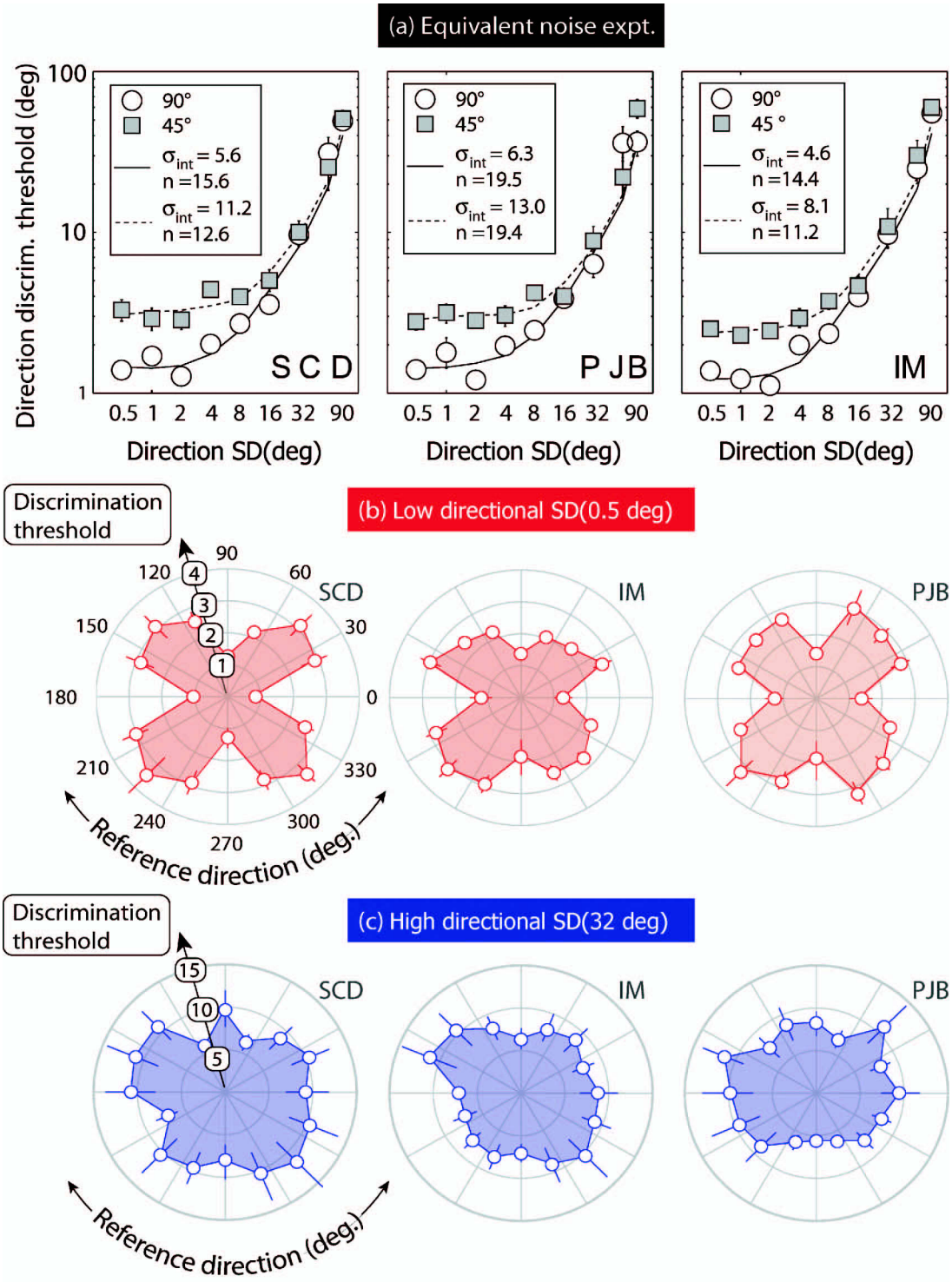

Figure 2. (a) Direction discrimination thresholds for patterns moving with a mean direction of 45° (filled squares) or 90° (open circles), plotted as a function of the range of directions present in the stimulus. Performance is poorer with oblique patterns at low directional *SD* but then converges at larger directional ranges. Fits of the EN model (solid and dashed lines) give estimates of local noise and global sampling (given in the legend as σ_{int} and *n* respectively) and reveal that the OEM is caused by local noise nearly doubling between cardinal and oblique conditions (while efficiency—the number of samples used—remained roughly constant). We next measured the dependence of OEM on directional range for reference directions around the clock. (b and c) In these plots radial distance indicates discrimination threshold (i.e., closer to the center indicates better performance) and angle indicates reference direction, for (b) low and (c) high directional ranges, respectively. Error bars show 95% confidence intervals on thresholds. A robust oblique effect is evident for all noncardinal directions at low levels of directional *SD* but is greatly attenuated as directional range broadens. Again, this is consistent with the OEM being due to anisotropies in local motion processing.

Switkes, Mayer, & Sloan, 1978). The latter result led us to ask if the concentration of energy in cardinal directions would lead to anisotropies in local directional bandwidth measured in natural movies, which might in turn influence the tuning of local motion detectors in the visual system. To address this issue, we conducted an analysis of directional statistics within a natural movie stimulus.

Scene analysis

Several studies have examined the *global* statistics of time-varying sequences of natural scenes. In particular Dong & Atick (1995) showed that global power depends on the inverse of temporal frequency mirroring the well-known $1/f^{\alpha}$ dependence of power on spatial frequency in static scenes (Field, 1987). More recently, we have analyzed time-varying image sequences (commercial and naturalistic movies) and report higher global motion energy at the cardinal directions (Bex, Dakin, & Mareschal, 2005). There is much less work on the *local* motion structure of natural scenes. However, Van Hateren & Ruderman (1998) have shown that independent components filters derived from small patches (12 pixel square, 12 frame sequences) sampled from movies of broadcast TV had similar spatiotemporal properties to simple cells in primary visual cortex. In this section, we examine the distribution of motion energy across directions in natural movies recorded at walking speed.

Stimuli

The stimuli employed in the movie analysis were drawn from 40 min of video recorded using a hand-held digital video camera (JVC GR-DVP5E). The recording was made while the experimenter walked through a park and several busy streets in central London. We employed stimuli filmed in man-made environments because these match the recent visual experience of our subjects. The film did not contain explicit zooming (the zoom was fixed at the minimum setting) or tracking but approximately followed head movements of the experimenter. Videos consisted of 720 × 576 pixel interlaced image sequences filmed at 24.75 frames per second. Movies were sampled with 24-bit precision and compressed using the DV codec. As a control, we also recorded the same walk using the same camera physically titled by 45°. We maintained this angle by monitoring a spirit level attached to the top of the camera. All movie sequences are available from the first author on request.

Analysis

Movies were transferred from the video camera to a desktop PC. Each frame was then de-interlaced and resized (along the *y*-axis and using bilinear interpolation) to make a 720 × 576 pixel movie running at 49.5 frames per second. One pixel in such an image corresponds to an angular subtense of 3.7 arcmin, so that each frame captures approximately 44 deg. × 35 deg. of a visual scene. We used the green channel as our estimate of luminance and disregarded the other channels to generate monochrome image sequences. We then performed local motion– energy analysis of short (four-frame) 64 pixel-square sequences drawn randomly in space and time from the 118,800 unique frames available. Because we were interested in local motion structure, these sequences were not resized versions of the whole image but were cut directly from the larger movie; each was therefore effectively an 80.8 ms. view of a 3.95 deg. square region of the visual scene. Ten thousand such sequences were analyzed.

We controlled for any artifactual changes in direction structure that might be introduced by our analysis in the following way. We minimized sampling artefacts due to the image raster by rotating each movie sequence through a random angle prior to analysis (and then later correcting for that initial random rotation). We also windowed patches by a 2D raised cosinusoidal window to minimize the contribution from the patch corners. Filter responses were later shifted to compensate for the initial rotation so that the possible initial random rotations ranged from 0° to 357.5° in steps of 2.5°, to match the peak sensitivities of the models' motion energy sensors. We calibrated this system with white noise movies and showed that the responses were flat across direction (within 1% of mean response). We also used filters tuned to relatively low spatial frequencies to minimize any artefacts in effective directional resolution that may result from image rescaling after de-interlacing. The departures from isotropy we report in the text must therefore be due to the statistics of our movie sequences.

The local motion analysis consisted of the following. Rotated and windowed image sequences were convolved with a bank of complex Gabor filters tuned to a wavelength of 16 pixels and quarter-cycle-per-frame motion. This filter is defined as:

$$g_\theta = \frac{1}{\sqrt{2\pi\sigma_x\sigma_y\sigma_t}} \exp\left[-\frac{x^2}{2\sigma_x^2} - \frac{y^2}{2\sigma_y^2} - \frac{t^2}{2\sigma_t^2} + i(\varpi_x x_\theta + \varpi_t t)\right], \quad (3)$$

where $x_\theta = x \cos\theta + y \sin\theta$ and the envelope parameters used were $\sigma_x = \sigma_y = 5.7$ pixels and $\sigma_t = 4$ frames (i.e., a the filter response was largely sustained over the four-frame sequence). We then compute direction–opponent motion energy by convolving an image sequence (I) with the filter at

direction θ and subtracting the response of the filter at direction $\theta + \pi$:

$$E_\theta(x,y,t) = \lfloor |I \otimes g_\theta| - |I \otimes g_{\theta+\pi}| \rfloor, \quad (4)$$

where $\lfloor x \rfloor$ is the half-squaring operation (Simoncelli & Heeger, 1998) $\lfloor f(x) \rfloor = \max(0, f(x))^2$.

To control for any anisotropies in directional structure that might have been present in the original movie sequence (e.g., due to image artefacts resulting from the DV codec, or anisotropic variation in directional sampling rates due to interlacing), we also ran an identical analysis on another movie sequence recorded with a camera physically tilted at 45°.

Results

Figure 3 gives the results from the computational analysis. Pooling the energy across all pixels within an image measures global directional energy (shown by the grey line in Figure 3i) and indicates that that there is substantially less energy on the oblique than on the cardinal axes. Notice that downwards motion dominates in our movie because of the downwards motion of the ground-plane—generated by ego motion—which tends to be more textured and of higher contrast than the upper visual field. We next conducted a local, pixel-by-pixel analysis of energy across directions. We noticed that the directional energy histograms were not always symmetrically distributed about the local mean direction and to quantify such asymmetries we fit local energy profiles with a Gaussian model with two independent (clockwise and anti-clockwise) *SD* parameters. The average best-fitting functions for various local mean directions are shown in Figure 3h. Note that information tends to be more tightly distributed around the cardinal direction (lower directional SDs), as highlighted by the red plot in Figure 3i, with bandwidth increasing rapidly from around 23° to around 36° as one moves away from the cardinal directions. Figure 3j plots the two sigma parameters as a function of the local mean direction and reveals eight points of symmetry (indicated by the small 'S's) on the cardinal axes and the "principle obliques" (cardinal directions ±45°). Asymmetry is maximal at the eight midpoints between the cardinal and principle obliques (i.e., 22.5°, 67.5°, etc.) where 1 *SD* can be up to 50% higher than the other. If the goal of sensory coding by the primary visual cortex is to produce a sparse distributed code of information present such substantial anisotropies in bandwidth and asymmetry of local directional information must be reflected in the tuning properties of visual neurons. We propose that this might in turn account for the essentially local nature of the OEM we have reported in the previous section.

An analysis of the movie sequences filmed from a tilted camera yielded results that were, when corrected for the 45° physical tilt, identical to those reported above. Therefore, directional anisotropies did not result from compression artefacts and anisotropies are unlikely to have been introduced by our analysis (recall that all movies also underwent random rotation prior to analysis to further preclude this possibility). In short we are confident that the anisotropies in local direction statistics we observe are a property of time-varying sequences of natural scenes.

Are these differences sufficient to explain the magnitude of the local deficit observed (i.e., an approximate doubling of threshold)? Figure 3k shows the response of a bank of channels (with characteristics similar to Figure 3h) to a series of stimuli containing a single direction, at 112.5°, 135°, 157.5°, and 180° (i.e., the preferred directions of the channels shown in Figure 3h). Notice that the combined effect of anisotropies in asymmetry and bandwidth has a profound effect on the response of the system as a whole. We now observe a strongly leptokurtic ("peaky") response from the cardinally tuned filter. If the precision of the local motion system is, as is widely believed, based on the derivative of the channel response, then this response will serve to further optimize the precision of the local directional signal.

Discussion

Relationship to previous findings

Gros et al. (1998) have reported an OEM for low and high levels of stimulus noise, whereas in this study we only find a measurable OEM at low levels of directional noise. We consider the likely explanation for this discrepancy to be due to the amount and type of noise employed. Our EN task requires observers to integrate all motion directions, whereas motion coherence requires observers to ignore dots that are not moving in the target direction, so there is no a priori reason to assume that the OEM would vary with noise level in motion coherence, especially over the relatively small range employed in their study (1/3*threshold level). Furthermore, we have argued that motion coherence paradigms cannot separate the effects of local and global noise (Dakin et al., 2005) because the presence of nonsignal dots not only dilutes the global motion signal but can also impede the visual systems ability to match corresponding elements between frames (Barlow & Tripathy, 1997). Therefore, whether it is local or global in origin, the OEM is to be expected at low and high noise levels within motion coherence paradigms.

Heeley et al. (1997) used EN with static filtered noise of various orientation bandwidths and report that elevated

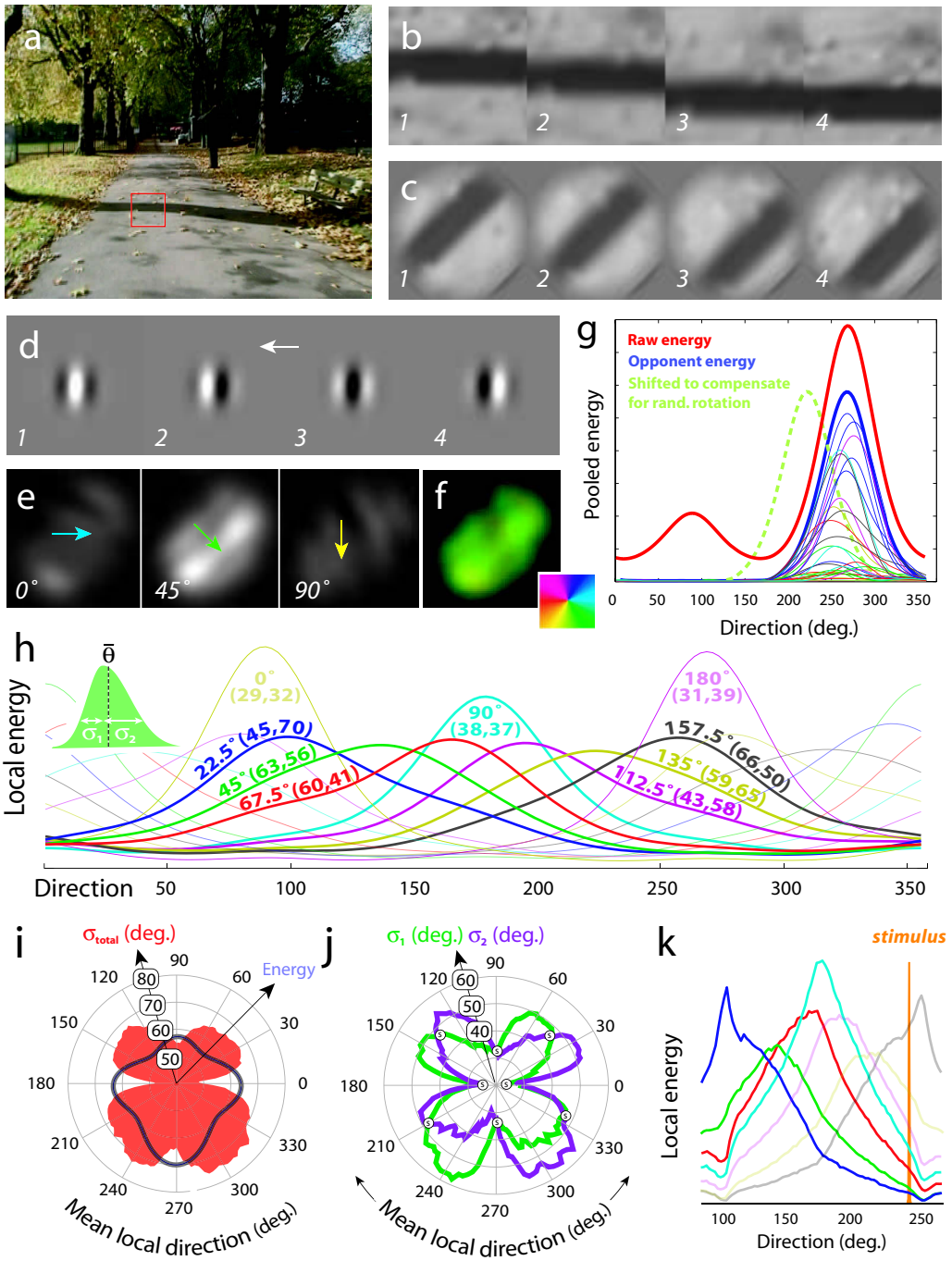

Figure 3. Local direction statistics of natural movies. (a) A single frame from a digital movie filmed from the point of view of an observer walking through an urban environment. Four stills from the framed region are shown in panel b. Our analysis consists of (c) randomly rotating a windowed-patch (to avoid image-raster artefacts), convolving the result with (d) motion–energy filters at various directions to give (e). We then compute pixel-by-pixel direction–energy histograms; (f) Mean local direction (insert shows the color code) computed from the histograms. (g) Opponent-motion energy (blue) is computed from raw energy (red) at one pixel; histograms are shifted to compensate for earlier random rotation. (h) Directional structure plotted for various local mean directions; curves are fits of the 2-σ Gaussian model (green inset); a sample of raw energy (gray circles) is shown. Energy is more broadly distributed around oblique directions (parameters—μ, σ_1, σ_2—are given), and with the exception of 45°, 135°, 225°, and 315° is asymmetrically distributed. (i) Gray line shows image power as a function of local direction and is dominated by the downwards motion of the ground-plane during ego-motion. Red area shows total directional *SD* and (j) thick lines, σ_1 and σ_2, as a function of local direction. The 'S' symbols mark points of symmetry about the mean. (k) The response of a filter bank, with the tuning characteristics shown in panel h, to a series of directionally punctate stimuli (e.g., drifting sine-wave) moving in the preferred direction of the channels shown in panel h. Differences in channel bandwidth and asymmetry lead to substantial differences in the distributions of response.

orientation discrimination thresholds along oblique axes were attributable both to an increase in internal noise and a reduced sampling efficiency. We consider this result likely to be attributable to a failure to test stimuli with sufficiently broad bandwidth. Figure 1d illustrates that the signature of a system limited by local noise is convergence of performance at high levels of external noise, so that the ability of EN to accurately assess sample size is crucially contingent on these high directional bandwidth conditions. In the earlier orientation study, the maximum orientation *SD* tested was 25° so that the highest threshold measured was <7°. Compare this to our own study where we tested directional *SD*s of 90° producing thresholds of the order of 40°–50°. One of the fundamental problems with assessing thresholds at very high levels of orientation or directional noise is that one must take into account wrapping in fitting psychometric functions if one is not to overestimate threshold. We describe how to do this elsewhere (Dakin et al., 2005).

Our finding that the OEM is due to the properties of local motion mechanisms also resolves and consolidates a number of existing findings in the substantial literature on the oblique effect:

1. It is consistent with the observed broader tuning of V1 neurons (Li et al., 2003), which are thought to subserve local motion perception.
2. V1 neurons are also thought to limit contrast detection thresholds (Ress & Heeger, 2003), so that their broader tuning bandwidths would lead to poorer detection of obliquely moving directions.
3. Direction discrimination in noise-free stimuli is dominated by limits on the precision of local mechanisms; therefore we expect poorer direction discrimination for suprathreshold, oblique, drifting sine-wave gratings.
4. While motion coherence thresholds are generally limited by both local and global constraints (as indicated above) at high (near-threshold) levels of noise the influence of local motion uncertainty will be minimized so that a system operating with similar integration efficiency for all directions, as described, predicts no elevation of motion coherence thresholds (Gros et al., 1998).
5. McMahon & MacLeod (2003) report that oblique gratings are more effective at masking (and inducing illusory tilt) and interpret their findings in terms of asymmetrical tuning for orientations off the cardinal and principle obliques. Inasmuch as our statistical analysis will be driven by local orientation as well as direction statistics, our findings are parsimonious with this view.

Additionally, reverse oblique effects have been observed (Essock, DeFord, Hansen, & Sinai, 2003; Wilson, Loffler, Wilkinson, & Thistlethwaite, 2001) for detection of high-contrast stimuli in noise. The explanations advanced have centered on the visual system compensating for the overrepresentation of horizontal and vertical information in natural scenes by incorporating anisotropic weighting into contrast gain control. We speculate that the variation in directional bandwidth we observe in natural images may cast light on these results. The stimuli that produce inverse oblique effects have broad orientation bandwidths (Glass patterns or natural images) and so superior performance can be achieved with broad bandwidth channels. At near-threshold contrasts, broad channels are insensitive because they integrate more noise, however at high contrasts, where detector noise no longer limits performance broad bandwidths integrate more signal.

How “local” is “local motion”?

Heeley & Buchanan-Smith (1992) report that direction discrimination thresholds for drifting plaids are determined by the plaid’s perceived direction and not by the direction of its components; that is, subjects were poorer at discriminating the direction of plaids that appeared to move in oblique directions but were composed of horizontal and vertical components than plaids composed of oblique components that appeared to move in a cardinal direction. This is an important result showing that the OEM does not operate at the level of the individual directionally tuned channels—responsible for signaling plaid component directions—but arises after combination of such filter outputs (or whatever visual processes underpin the perception of two-dimensional motion in such patterns). This result might be seen as contradictory to our own because it implies a late locus for the OEM within the visual motion processing hierarchy. However, we believe that our results are not incompatible. EN shows that the OEM arises at the level of the motion of individual elements and we have called that a local motion limit: in showing the effect is not at the level of pooled motion (across space) we are effectively imposing a top–down limit on where the effect arises. Heeley & Buchanan-Smith (1992) have shown that the OEM arises after low-level filter combination. This is a bottom-up limit; OEM cannot arise at or prior to component motion coding. A parsimonious interpretation of these two results is that OEM arises at the level of local two-dimensional motion processing. This raises the issue of the neural site of local motion computation. Physiological evidence showing cells in V1 do not compute 2D pattern motion (specifically plaid direction; Movshon, Adelson, Gizzi, & Newsome, 1985) would therefore appear to force the locus of local motion processing out of V1. We think that drawing such a conclusion would be premature for two reasons. First several models of motion perception, including gradient methods (e.g., Johnston et al., 1999) and more recent proposals

involving divisive center-surround gain control, are able to compute two-dimensional plaid motion locally, in a manner that could be implemented using V1 circuitry. Second, recent electrophysiological evidence (Guo, Benson, & Blakemore, 2004) suggests around 10% of V1 cells are pattern selective in awake (but not anaesthetized) preparations. These results suggest that the cortical locus of two-dimensional/plaid motion remains far from certain.

Predictions

Based on our findings, we make two predictions for electrophysiology. First, there should be no significant anisotropies in the number, tuning, or noise properties in the motion-tuned neurons in higher areas of the visual cortex (e.g., MT, MST). Second, closer inspection of the response properties of motion-tuned neurons in primary visual cortex should reveal differences in the directional bandwidth, and skew of their tuning for cardinal and obliquely tuned stimuli.

Acknowledgments

This research was supported by the BBSRC (31/S17766). We are grateful to the anonymous reviewers for their comments.

Commercial relationships: none.
Corresponding author: Steven Dakin.
Email: s.dakin@ucl.ac.uk.
Address: Institute of Ophthalmology, University College London, 11-43 Bath Street, London EC1V 9EL, UK.

References

Appelle, S. (1972). Perception and discrimination as a function of stimulus orientation: The "oblique" effect in man and animals. *Psychological Bulletin, 78,* 266–278. [PubMed]

Baddeley, R. J., & Hancock, P. J. (1991). A statistical analysis of natural images matches psychophysically derived orientation tuning curves. *Proceedings of the Royal Society of London. Series B, Biological Science, 246*(1317), 219–223. [PubMed]

Barlow, H. (1980). The absolute efficiency of perceptual decisions. *Philosophical Transactions of the Royal Society of London, B290,* 71–82. [PubMed]

Barlow, H., & Tripathy, S. P. (1997). Correspondence noise and signal pooling in the detection of coherent visual motion. *Journal of Neuroscience, 17*(20), 7954–7966. [PubMed] [Article]

Betsch, B. Y., Einhauser, W., Kording, K. P., & Konig, P. (2004). The world from a cat's perspective—Statistics of natural videos. *Biological Cybernetics, 90*(1), 41–50. [PubMed]

Bex, P. J., Dakin, S. C., & Mareschal, I. (in press). Critical band masking in optic flow. *Network.*

Brainard, D. H. (1997). The Psychophysics Toolbox. *Spatial Vision, 10,* 433–436. [PubMed]

Coppola, D. M., Purves, H. R., McCoy, A. N., & Purves, D. (1998). The distribution of oriented contours in the real world. *Proceedings of the National Academy of Sciences of the United States of America, 95*(7), 4002–4006. [PubMed] [Article]

Craven, B. J. (1993). Orientation dependence of human line-length judgements matches statistical structure in real-world scenes. *Proceedings of the Royal Society of London. Series B, Biological Sciences, 253*(1336), 101–106. [PubMed]

Dakin, S. C., Mareschal, I., & Bex, P. J. (2005). Local and global limitations on direction integration assessed using equivalent noise analysis. *Vision Research, 45,* 3027–3049. [PubMed]

Dong, D. W., & Atick, J. J. (1995) Statistics of time-varying images. *Network, 6,* 345–358.

Essock, E. A., DeFord, J. K., Hansen, B. C., & Sinai, M. J. (2003). Oblique stimuli are seen best (not worst!) in naturalistic broad-band stimuli: A horizontal effect. *Vision Research, 43*(12), 1329–1335. [PubMed]

Field, D. J. (1987). Relations between the statistics of natural images and the response properties of cortical cells. *Journal of the Optical Society of America, A4,* 2379–2394. [PubMed]

Flinn, J. T., & Watamaniuk, S. N. J. (1997). The oblique effect for motion. *Investigative Ophthalmology Visual Science, 38*(4), S379.

Furmanski, C. S., & Engel, S. A. (2000). An oblique effect in human primary visual cortex. *Nature Neuroscience, 3*(6), 535–536. [PubMed]

Gros, B. L., Blake, R., & Hiris, E. (1998). Anisotropies in visual motion perception: A fresh look. *Journal of the Optical Society of America. A, Optics Image Science, and Vision, 15*(8), 2003–2011. [PubMed]

Guo, K., Benson, P. J., & Blakemore, C. (2004). Pattern motion is present in V1 of awake but not anaesthetized monkeys. *European Journal of Neuroscience, v19,* 1055–1066. [PubMed]

Hancock, P. J., Baddeley, R. J., & Smith, L. S. (1992). The principal components of natural images. *Network: Computational Neural Systems, 3,* 61–71.

Hansen, B. C., Essock, E. A., Zheng, Y., & DeFord, J. K. (2003). Perceptual anisotropies in visual processing and their relation to natural image statistics. *Network, 14*(3), 501–526. [PubMed]

Heeley, D. W., & Buchanan-Smith, H. M. (1992). Directional acuity for drifting plaids. *Vision Research, 32*(1), 97–104. [PubMed]

Heeley, D. W., Buchanan-Smith, H. M., Cromwell, J. A., & Wright, J. S. (1997). The oblique effect in orientation acuity. *Vision Research, 37*(2), 235–242. [PubMed]

Johnston, A., McOwan, P. W., & Benton, C. P. (1999). Robust velocity computation from a biologically motivated model of motion perception. *Proceedings of the Royal Society of London. Series B, Biological Science, 266*(1418), 509–518.

Keil, M. S., & Cristobal, G. (2000). Separating the chaff from the wheat: Possible origins of the oblique effect. *Journal of the Optical Society of America. A, Optics Image Science, and Vision, 17*(4), 697–710. [PubMed]

Li, B., Peterson, M. R., & Freeman, R. D. (2003). Oblique effect: A neural basis in the visual cortex. *Journal of Neurophysiology, 90*(1), 204–217. [PubMed] [Article]

McMahon, M. J., & MacLeod, D. I. (2003). The origin of the oblique effect examined with pattern adaptation and masking. *Journal of Vision, 3*(3), 230–239, http://journalofvision.org/3/3/4/, doi:10.1167/3.3.4. [PubMed] [Article]

Movshon, J. A., Adelson, E. H., Gizzi, M. S., & Newsome, W. T. (1985) The analysis of moving visual patterns. In C. Chagas, R. Gattass, & C. G. Gross (Eds.), *Study group on pattern recognition mechanisms. Pontifica Academia Scientiarum, Vatican City,* 117–151.

Ress, D., & Heeger, D. J. (2003). Neuronal correlates of perception in early visual cortex. *Nature Neuroscience, 6*(4), 414–420. [PubMed]

Simoncelli, E. P., & Heeger, D. J. (1998). A model of neuronal responses in visual area MT. *Vision Research, 38*(5), 743–761. [PubMed]

Switkes, E., Mayer, M. J., & Sloan, J. A. (1978). Spatial frequency analysis of the visual environment: Anisotropy and the carpentered environment hypothesis. *Vision Research, 18*(10), 1393–1399. [PubMed]

Van Hateren, J. H., & Ruderman, D. L. (1998) Independent component analsysis of natural image sequences yields spatio-temporal filters similar to simple cells in primary visual cortex. *Proceedings of the Royal Society of London. Series B, Biological Science, 265*(1412), 2315–2320. [PubMed]

Watamaniuk, S. N., & Heinen, S. J. (1999). Human smooth pursuit direction discrimination. *Vision Research, 39*(1), 59–70. [PubMed]

Watt, R. J., & Andrews, D. (1981). APE: Adaptive probit estimation of psychometric functions. *Current Psychological Review, 1,* 205–214.

Watt, R. J., & Morgan, M. J. (1983). The recognition and representation of edge blur: Evidence for spatial primitives in human vision. *Vision Research, 23*(12), 1465–1477. [PubMed]

Wilson, H. R., Loffler, G., Wilkinson, F., & Thistlethwaite, W. A. (2001). An inverse oblique effect in human vision. *Vision Research, 41*(14), 1749–1753. [PubMed]